3-Mercaptopropyltrimethoxysilane as a Cu corrosion inhibitor in KCl solution

R. TREMONT[1], H. De JESÚS-CARDONA[2], J. GARCÍA-OROZCO[1], R.J. CASTRO[3] and C.R. CABRERA[1*]

[1]*Department of Chemistry, P.O. Box 23346, University of Puerto Rico, Río Piedras Campus, San Juan, PR 00931-3346*

[2]*Department of Chemistry, University of Puerto Rico, Bayamón Technological University College, Bayamón, PR 00959-1919*

[3]*Department of Chemistry, University of Puerto Rico, Cayey University College, Cayey, PR 00736*
(*author for correspondence)

Abstract

3-mercaptopropyltrimethoxysilane (MPS) has been used as a copper corrosion inhibitor in 0.100 mol L^{-1} KCl solution. The inhibition was studied as a function of the MPS pretreatment concentration in ethanol. The MPS concentration used was between 1.0×10^{-8} mol L^{-1} and 1.0×10^{-1} mol L^{-1}. A freshly-cleaned Cu electrode was inserted in an ethanolic solution of MPS for 30 min for pretreatment, and was then exposed to a 0.100 mol L^{-1} KCl aqueous solution for 1 h. From the polarization resistance, the inhibition efficiency improved with increase in MPS concentration during the pretreatment. The MPS adsorption on Cu followed a Langmuir adsorption behaviour. However, at MPS concentrations larger than 1.0×10^{-4} mol L^{-1} the inhibition decreased. Moreover, the inhibition efficiency decreased with increase in the exposure time of the MPS modified Cu electrode in the KCl aqueous solution. Polarization studies suggest that MPS is an anodic as well as a cathodic inhibitor, in the presence of dissolved oxygen. X-ray photoelectron spectroscopy (XPS) analysis of the Cu samples showed that the organic compound modifies the Cu surface and scanning electron microscopy (SEM) studies indicated that MPS protects the Cu surface when exposed for 350 h to laboratory environment. Polarized grazing angle Fourier transform-infrared (FTIR) microscopy analysis determined the presence of a polymer on the Cu surface.

1. Introduction

A large number of organic compounds are known to be applicable as corrosion inhibitors for copper. However, only a few compounds have been thoroughly investigated [1]. Thiol (R-SH) molecules have been studied as possible metal corrosion inhibitors. For example, in the case of iron [2], alcanethiols $[CH_3(CH_2)_n SH]$ have been shown to be good corrosion inhibitors in methanol solutions of $LiClO_4$ and in the presence of $FeCl_3$. Some thiol derivatives of 2-mercaptobenzymidazol [3–8] have given good results on steel, in HCl and H_2SO_4 solutions and at different temperatures. In this case the chemisorption followed a Langmuir isotherm behaviour. On the other hand, orthoaminothiophenol [9] was shown to be a good corrosion inhibition for nickel in 3% NaCl solution.

For the protection of copper, it has been found that benzenethiol [10] and some substituted benzenethiols, through polymerization of the thiols on the metal surface, are very effective inhibitors in acid and alkaline solutions. In addition, tetrazol and derivatized triazol [11, 12] have been used as corrosion inhibitors for copper in saline solutions of Na_2SO_4, $NaNO_3$, $NaClO_4$ and NaCl, at low pH. Other materials used for this purpose are the alcanethiols, which show chemisorption and formation of a monolayer over copper surfaces [13–23]. It is clear that 2-mercaptobenzothiazole protects copper and its alloys against corrosion in acid solution [24, 25]. Trabanelli attributed this behaviour to a surface film [26]. Another environment used to study the behaviour of 2-mercaptobenzothiazole was ethanolic media. The formation of a polymeric complex with copper(I) and ionized thiols was demonstrated [27]. Self-assembled monolayer formation at copper with 11-mercapto-1-undecanol, 1,2-bis(trichlorosilyl)ethane and octadecyltrichlorosilane have also been recently identified [28, 29].

The chemisorption of alcanethiols on copper is practiced [30, 31]. Long chain alcanethiols are effective in promoting discreet condensation on copper condenser tubes. These materials are effective inhibitors for copper corrosion [32], due to the effective blockage of the film for redox active electrochemical processes [33–35].

The 3-mercaptopropyltrimethoxysilane (MPS) molecule has a thiol as functional head group (Figure 1),
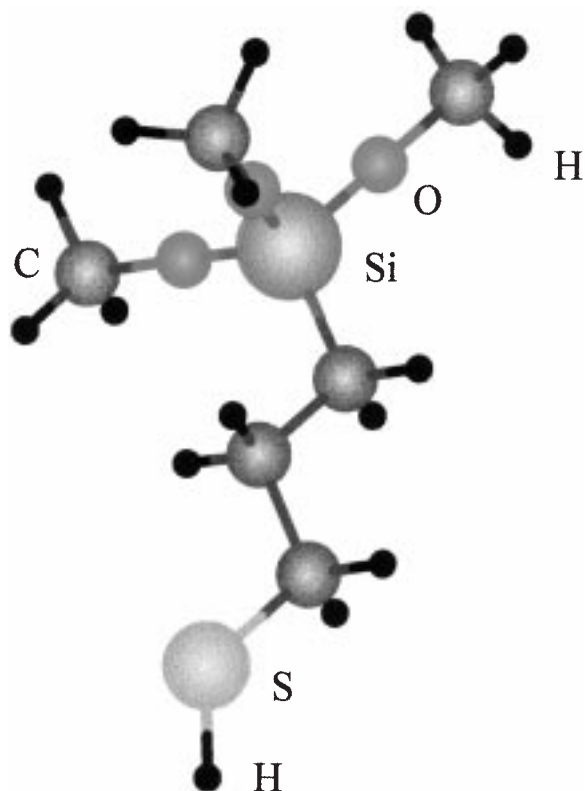
Fig. 1. Structure of 3-mercaptopropyltrimethoxysilane.

which forms a strong covalent bond with different metals [36, 39]. The end group of MPS is trimethoxysilane, which has three methoxy functional groups. Here, we present an alcanethiol with a protective silane group as a very effective protector of metallic surfaces [37–39] against corrosion. In the present study, MPS has been used as a copper corrosion inhibitor in KCl solutions. Corrosion inhibition has been studied by applying polarization curves, polarization resistance measurements, X-ray photoelectron spectroscopy (XPS) and scanning electron microscopy (SEM).

2. Experimental details

Sheets of Cu foil 1.0 mm in thickness (Aldrich, 99.98%) and 1 cm^2 in area were used in all experiments. Before use, the sheets were mechanically polished with silicon carbide belts (from 240 grit to 600 grit, Buehler), rinsed with nanopure water (18 MΩ cm in resistivity), polished with diamond paste (1 μm, Buehler) on microcloth polishing cloth (Buehler), rinsed with acetone (Aldrich) and dried under nitrogen. Finally, the freshly polished electrodes were pretreated before each experiment by cleaning with 10% HCl (Aldrich) for 30 s and washing with nanopure water.

For some experiments the Cu electrode surface was modified by immersion in a 30 mL ethanol solution at different MPS (95%, Aldrich) concentrations, between 1.0×10^{-1} mol L^{-1} and 1.0×10^{-7} mol L^{-1}. The Cu metal was placed in these solutions for 30 min. The

surfaces were then rinsed with ethanol and nanopure water, dried under nitrogen, and immerse in a 0.100 mol L^{-1} KCl solution for 1 h. To determine the optimum MPS concentration for Cu pretreatment, we varied the exposure time of the metal in contact with the best ethanolic solution of MPS up to three hours and the exposure time of the MPS modified Cu metal in the KCl solution up to 48 h.

The temperature in all the experiments was $23.6 \pm 0.1\,^{\circ}$C, and the KCl solutions had a pH of 6.3. The analyses were done in the presence of air.

The electrochemical measurements were performed in a conventional three electrode electrochemical cell, consisting of a platinum electrode, an auxiliary electrode and a saturated calomel electrode (SCE), as reference. A Princeton Applied Research (PAR) 273A potentiostat/galvanostat, controlled with the PAR 270 Research Electrochemistry Software installed in a personal computer, was used.

The X-ray photoelectron spectroscopy (XPS) analyses presented in this work were performed using a PHI 5600ci spectrometer. For the XPS measurements the samples were mounted over a stainless steel stopper using a molybdenum mask to assure good electrical contact. The sample analyses were done using a MgK_α X-ray source at 15.0 kV and 400 W. This instrument was equipped with a hemispherical analyser. The pass energy used was 93 eV for the survey analysis and 11 eV for the high resolution studies. All the analyses were performed at a pressure below 1×10^{-8} torr. The binding energy (BE) values were corrected using the C 1s signal of the atmospheric contaminants (BE = 285.0 eV).

The grazing angle FTIR microscopy experiments were carried out using a Nicolet Magna IR 750 with a NicPlan microscope. An incidence angle of 86°, between the *p*-plane of polarized light and the sample surface, was used. Characteristic FTIR spectra were obtained at a resolution of 4 cm^{-1}, with 10 000 scans and using a gold mirror as the background.

The scanning electron microscopy (SEM) analyses were performed using a Jeol JSM-5800LV with an accelerating voltage between 15.0 kV and 20 kV. Samples were attached on top of an aluminum stopper by means of 3M carbon conductive adhesive tape (SPI).

3. Results and discussion

3.1. *Effect of MPS concentration for corrosion inhibition*

Polarization curves were obtained to characterize the protection efficiency of MPS, where the potential sweep rate was 1 mV s^{-1}. The data were analysed using Tafel plots in the region of the corrosion potential, ±300 mV. For example, Figure 2 show the polarization curves for Cu in 0.100 mol L^{-1} KCl solution, with different concentrations of MPS. The inhibition effect is notable in the anodic and cathodic polarization regions with a

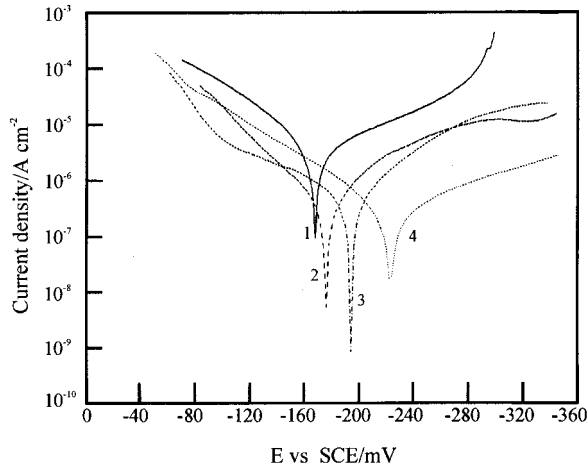Fig. 2. Potentiodynamic curves of a Cu electrode in 0.100 mol L^{-1} KCl at different concentrations of MPS pretreatment and at 23.6 °C. (1) Without MPS pretreatment; (2) 1.0×10^{-7} mol L^{-1} MPS; (3) 1.0×10^{-2} mol L^{-1} MPS and (4) 1.0×10^{-4} mol L^{-1} MPS.

cathodic displacement of the corrosion potential. This behaviour is due to the presence of the inhibitor on the copper surface. From Figure 2 we can obtain the current density for corrosion by extrapolating the Tafel line to the corrosion potential. The corrosion inhibition efficiency, E, was found from the following equation:

$$E = \left(\frac{i_o - i}{i_o} \right) \times 100 \qquad (1)$$

where i and i_o are the corrosion current densities with and without inhibitor, respectively.

Figure 3 shows the variation in corrosion inhibition efficiency with respect to log[C_{MPS}]. The efficiency increases with increase in inhibitor concentration, achieving a maximum of 95% at a MPS concentration of 1.0×10^{-4} mol L^{-1}.

Values of corrosion potential (E_{corr}), corrosion current density (i_{corr}), efficiency (E) and polarization resistance (R_p), as a function of MPS concentration in aqueous 0.100 mol L^{-1} KCl solution are presented in Table 1.
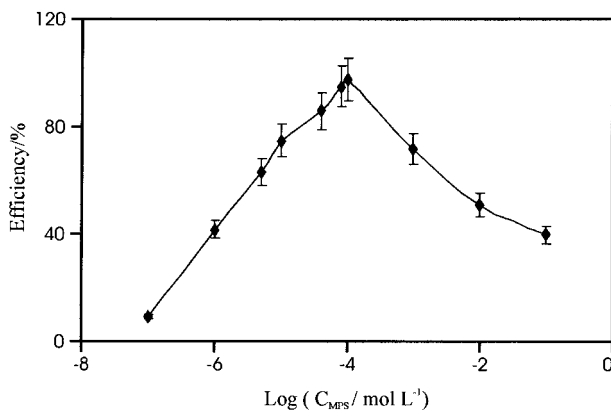
Table 1. Potentiodynamic data for the effect of MPS concentration on the corrosion inhibition of copper in 0.100 mol L^{-1} KCl solution at 23.6 °C

MPS concentration /mol L^{-1}	E_{corr} /V vs SCE	I_{corr} /μA cm^{-2}	Efficiency, E /%	R_p /kΩ cm^2
0	−168	6.0	–	17
1.0×10^{-7}	−177	5.0	9	19
1.0×10^{-6}	−188	3.0	42	29
5.0×10^{-6}	−195	2.0	63	36
1.0×10^{-5}	−200	1.2	75	42
4.0×10^{-5}	−209	0.70	86	49
8.0×10^{-5}	−220	0.30	95	59
1.0×10^{-4}	−224	0.10	98	73
1.0×10^{-3}	−208	0.50	90	39
1.0×10^{-2}	−194	1.4	72	32
1.0×10^{-1}	−189	2.0	61	25

Polarization resistance measurements were carried out at different MPS concentrations. Figure 4 shows the variation of the polarization resistance (R_p) against log[C_{MPS}], where R_p was determined from a plot of E(V) against I ($R_p = \Delta E / \Delta I$). From Figure 4, we see that an increase in MPS concentration produces an increase in the resistance to charge transfer between the solution and the metallic surface. The highest resistance was at a MPS concentration of 1.0×10^{-4} mol L^{-1} (Table 1).

3.2. *Effect of exposure time*

The effect of exposure time of the metal to the ethanolic solution of MPS was performed at a C_{MPS} of 1×10^{-4} mol L^{-1}. The exposure time was varied between 30 and 180 min. The modified Cu plate was then placed in 0.100 mol L^{-1} KCl solution, for 1 h.

Figure 5 shows Tafel plots at different pretreatment conditions. An increase in exposure time produced a decrease in exchange current density. However, at exposure times greater than 30 min, a slow increase exchange current density was found. Desorption of the inhibitor was probably occurring with time in the presence of the high concentration of chloride ion.
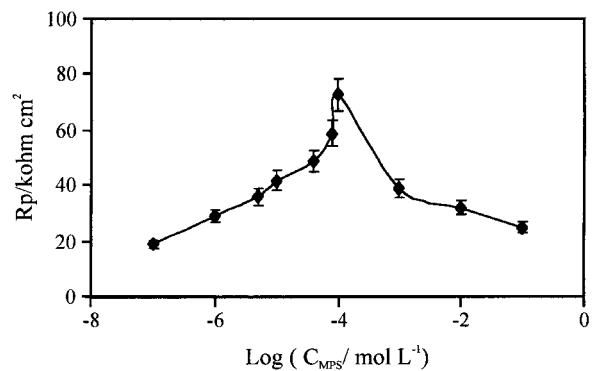

Fig. 3. Copper corrosion inhibition efficiency (E) in 0.1 mol L^{-1} KCl at 23.6 °C, as a function of log[C_{MPS}]. The C_{MPS} (mol L^{-1}) is the MPS concentration used in the pretreatment of Cu.

Fig. 4. Variation of the charge transfer resistance (R_p) as a function of the log[C_{MPS}], in 0.100 mol L^{-1} KCl solution. C_{MPS} (mol L^{-1}) is the MPS concentration used in the pretreatment of Cu.
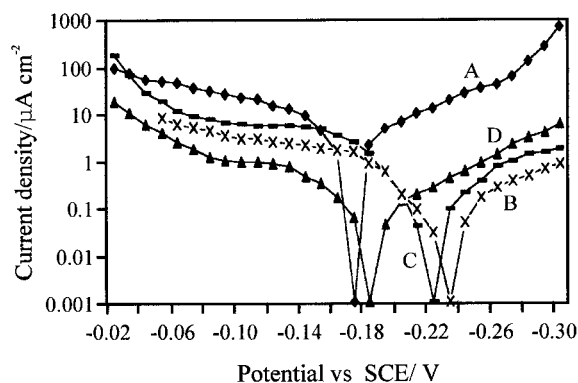
Fig. 5. Tafel behaviour of a Cu electrode in 0.100 mol L^{-1} KCl aqueous solution as a function of the pretreatment time of Cu in a 1.0 × 10^{-4} mol L^{-1} MPS ethanolic solution: (A) without MPS pretreatment; in the MPS solution for (B) 30 min, (C) 60 min and (D) 180 min.

Figure 6 shows polarization curves for the Cu electrodes modified in a solution of 1.0 × 10^{-4} mol L^{-1} MPS. After the first hour of exposure to the KCl solution, the corrosion potential shifted 20 mV in the

negative direction (Figure 6(A)) when compared to what was observed without the inhibitor. In addition, the current density increased with further exposure, and the corrosion potential shifted towards a more negative value and later moved in the positive potential direction. This could be an effect associated with the formation of an anionic product of the electron transfer reaction occurring at the Cu surface. A small increase in the corrosion current density was also observed. This is in accordance to what has been observed by Beccaria and collaborators [40].

3.3. *Application of the Langmuir adsorption isotherm*

The adsorption of MPS on Cu was modeled by using the Langmuir isotherm equation,

$$\theta = \frac{KC}{1 + KC} \tag{2}$$

where C is concentration, K is a constant and θ is the surface coverage which is also given by,
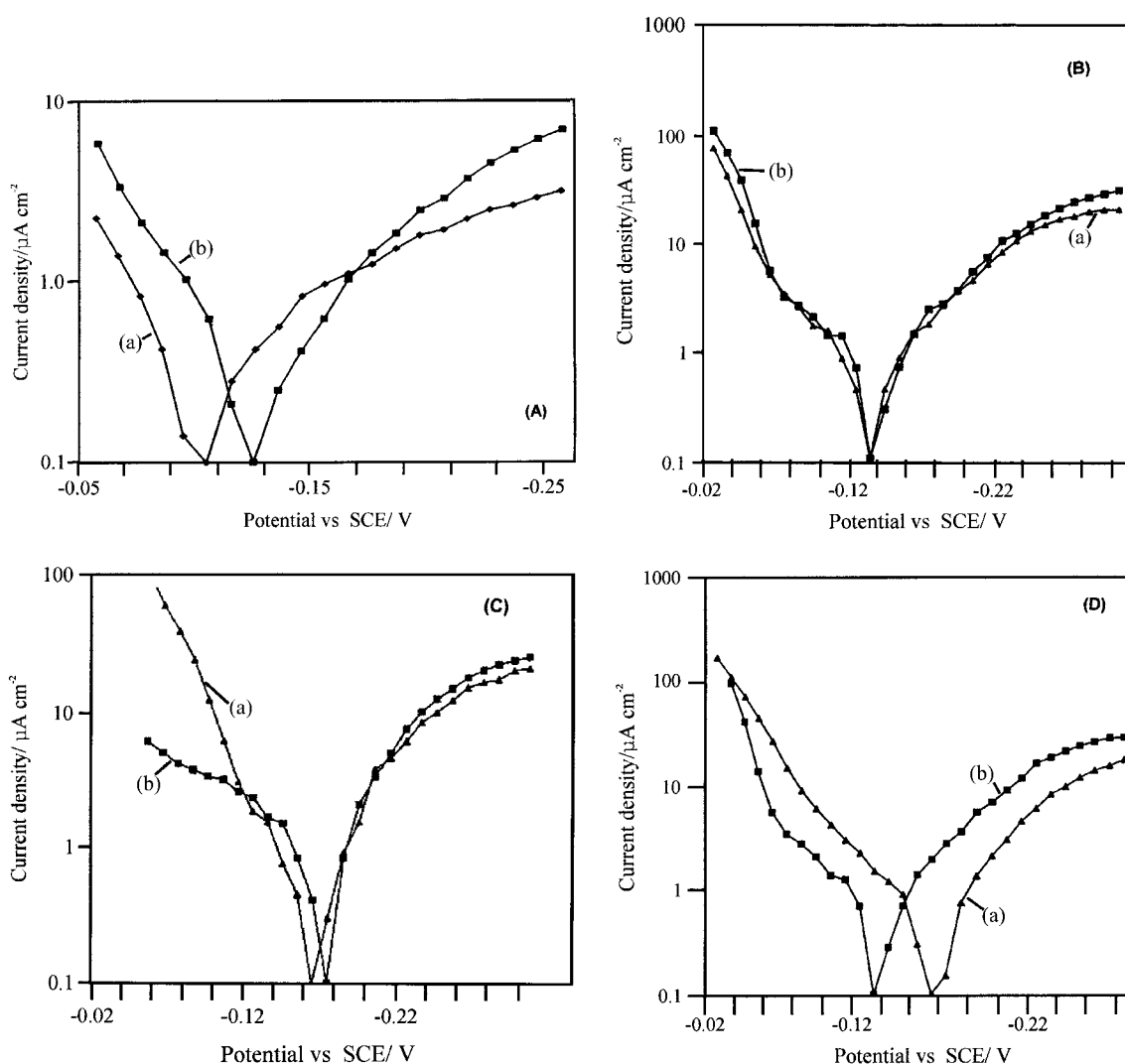

Fig. 6. Tafel behaviour of Cu metal that was pretreated for 30 min in an ethanolic solution of 1.0 × 10^{-4} mol L^{-1} MPS and posttreated in 0.100 mol L^{-1} KCl solution at different exposure times. (a) Without MPS and (b) with MPS pretreatment at exposure times in KCl solution for: (A) 1, (B) 4, (C) 24 and (D) 48 h.

$$\theta = \frac{E}{100} \qquad (3)$$

A plot of $\log(\theta/1 - \theta)$ against $\log(C)$, was used to test for Langmuir behaviour of Equation 2. The efficiency (E) was calculated using Equation 1 [41, 42].

The experimental data (Figure 7) closely follows a Langmuir adsorption isotherm behavior. From the value of K (the ordinate-intercept in Figure 7) we can calculate the free energy of adsorption of MPS on Cu, knowing that [42]:

$$K = A \exp\left(\frac{-\Delta G}{RT}\right) \qquad (4)$$

where A is 1/(solvent concentration). In our case the ethanol concentration was 15.52 mol L^{-1}. The free energy of adsorption of MPS was found to be -35 kJ mol^{-1}. This value is lower than the ΔG of -184 kJ mol^{-1}, which has been presented by Dubois and Nuzzo for the bond strength between Au and a thiolate molecule [43]. We attribute this discrepancy to the type of interaction that can take place between the thiol molecule and the Cu or Au surface.

3.4. Surface analysis studies

The X-ray photoelectron spectroscopy (XPS) analysis of the Cu surface, pretreated with different MPS concentrations and with different exposure times to KCl solutions, indicated that the quantity of Cu^{2+} that was formed on the surface decreased with the MPS pretreatment. Table 2 presents the area ratio of the Cu satellite peak to the Cu 2p$_{3/2}$ main binding energy peak. This ratio is a parameter directly proportional to the quantity of Cu^{2+} present on the surface. Clearly, this indicates that the quantity of Cu^{2+} was greater on the sample of Cu that had no pretreatment with MPS.

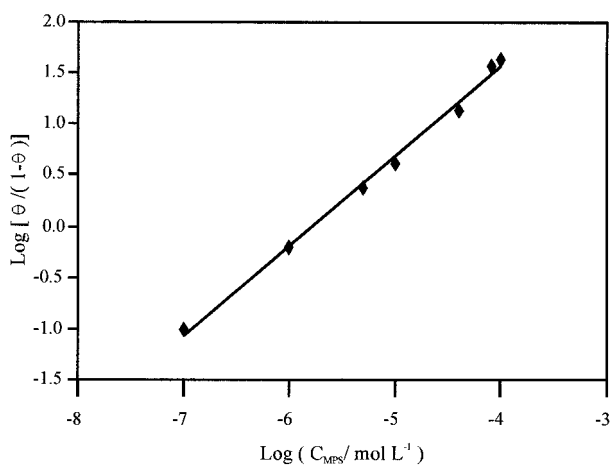Polarized grazing angle Fourier transform-infrared (FTIR) microscopy analysis of the Cu surface pretreated

Table 2. Area ratio of the Cu 2p$_{3/2}$ (Cu$_s$) satellite peak to the Cu 2p$_{3/2}$ (Cu$_p$) main XPS peak for Cu samples which were exposed to a 0.100 mol L^{-1} KCl solution

Sample of Cu	(Cu$_s$)/(Cu$_p$)
Without MPS	0.13
With MPS	0.06

with 1.0×10^{-4} mol L^{-1} MPS and with 1 h exposure to 0.100 mol L^{-1} KCl solution (Figure 8(A) and (B)), indicated the presence of a polymer on the Cu surface [44–49]. There was a decrease of the —SiOCH$_3$ and —SiOC IR signals and the presence of a new —Si—O—Si— signal [50]. This could be due to the presence of unpolymerized MPS molecules or —SiOCH$_3$ defects in the polymer. Furthermore, the —SH signal was never observed, which suggest that the MPS chemisorbs to Cu surface through the sulfur atom, without an R—S—S—R (550–430 cm^{-1}) signal.

Scanning electron microscopy of the copper surface, with and without MPS and exposed to the laboratory environment (25 °C) for 350 h, were taken to determine
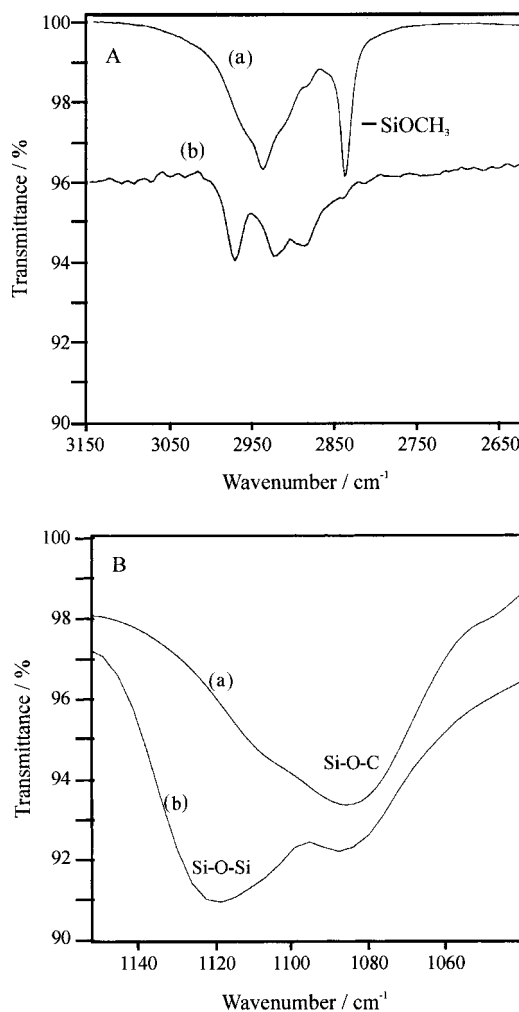

Fig. 7. Langmuir adsorption isotherm of MPS on copper (calculated from i_o that were determined from Tafel plot measurements in 0.100 mol L^{-1} KCl solution).

Fig. 8. Fourier transform infrared (FTIR) spectra of: (a) the MPS molecule and (b) Cu surface pretreated with MPS and exposed to a 0.100 mol L^{-1} KCl solution for 1 h. (A) —SiOCH$_3$ band; (B) Si—O—Si and Si—O—C bands.

microscopically the MPS protection. Figure 9(a) and (b) show the SEM images of the protected and unprotected surface, respectively. We can appreciate the very good protection of the copper surface by the MPS molecule. The Cu surface without MPS modification exhibits attack by the KCl solution with the formation of various pits. On the other hand, the surface of copper that contained MPS molecules showed a smooth surface with very few pits.

4. Conclusions

The organic molecule, MPS, can modify the Cu surface and inhibit corrosive attack in a 0.100 mol L^{-1} KCl solution. The optimum concentration for MPS protection of Cu was 1.0×10^{-4} mol L^{-1} at room temperature. The effect of MPS protection decreases with exposure time in 0.100 mol L^{-1} KCl. The XPS results support the idea that MPS modified the Cu surface and inhibited corrosion. Results of polarized grazing angle Fourier transform infrared (FTIR) microscopy analysis indicated the presence of a polymer on the Cu surface. The FTIR results also suggest that MPS chemisorption on the Cu surface be through the sulfur atom.
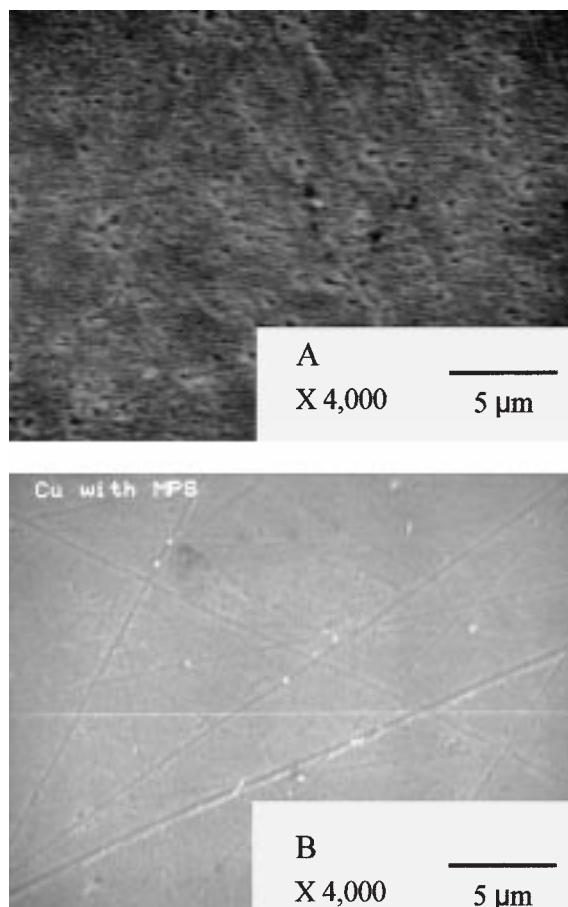

Fig. 9. Scanning electron micrographs (4000×) of a copper surface after exposure to a 0.100 mol L^{-1} KCl solution, for 350 h, at 25 °C, (A) without MPS pretreatment and (B) with MPS pretreatment.

References

1. G. Trabanelli, *in* F. Mansfeld (Ed.), 'Corrosion Mechanisms' (Marcel Dekker, New York, 1987), p. 119.
2. K. Tatsuya, N. Hiroshi and A. Kunitsugu, *J. Electrochem. Soc.* **143** (1996) 3866.
3. A.N. Starchak, A.N. Krasovskii, V.A. Anishchenko and L.D. Kosukhina, *Zashch. Met.* **30** (1994) 405.
4. M. Th. Makhlouf, S.A. El-Shatory and A. El-Said, *Mater. Chem. Phys.* **43** (1996) 76.
5. M. Th. Makhlouf and M.H. Wahdan, *Pol. J. Chem.* **69** (1995) 1072.
6. M. Th. Makhlouf, M.H. Wahdan and M. Hassan, *ACH-Models Chem.* **132** (1995) 903.
7. M.H. Wahdan, *Mater. Chem. Phys.* **49** (1997) 135.
8. Y.I. Mikshis, L.A. Rastenite and A.I. Rutavichus, *Pot. Met.* **33** (1997) 288.
9. A. Srhiri, Y. Derbali and T. Picaud, *Corrosion* **51** (1995) 788.
10. S. Sankarapapavinasam and M.F. Ahmed, *J. Appl. Electrochem.* **22** (1995) 390.
11. G. Brunoro, A. Frignani and L. Tommesani, *Ann. Univ. Ferrara, Sez. V, Suppl.* 10, (1995), p. 1053.
12. K. Mori and Y. Nakamura, *J. Polym. Sci. Polym. Let. Ed.* **21** (1983) 889.
13. D.L. Seymour, S. Bao, C.F. McConville, M.D. Crapper, D.P. Woodruff and R.G. Jones, *Surf. Sci.* **189/190** (1987) 529.
14. J.Y. Gui, D.A. Stern, D.G. Frank, F. Lu, D.C. Zapien and A. Hubbard, *Langmuir* **7** (1991) 955.
15. J. Uehara and K. Aramaki, *J. Electrochem. Soc.* **138** (1991) 3245.
16. M.D. Porter, T.B. Bright, D.L. Allara and C.E.D. Chidsey, *J. Am. Chem. Soc.* **109** (1987) 3559.
17. G.M. Whitesides and P.E. Laibinis, *Langmuir* **6** (1990) 87.
18. M.M. Walczak, C. Chung, S.M. Stole, C.A. Widrig and M.D. Porter, *J. Am. Chem. Soc.* **113** (1991) 2370.
19. C.A. Widrig, C. Chung and M.D. Porter, *J. Electroanal. Chem.* **310** (1991) 335.
20. S.M. Stole and M.D. Porter, *Langmuir* **6** (1990) 1199.
21. P.E. Laibinis, G.M. Whitesides, D.L. Allara, Y.T. Tao, A.N. Parikh and R.G. Nuzzo, *J. Am. Chem. Soc.* **113** (1991) 7152.
22. P.E. Laibinis and G.M. Whitesides, *J. Am. Chem. Soc.* **114** (1992) 1990.
23. L.C.F. Blackman and M.J.S. Dewar, *J. Chem. Soc.* **171** (1990) 1957.
24. M. Musiani M.G. Mengoli, M. Fleischmann and R.B. Lowry, *J. Electroanal. Chem.* **217** (1987) 187.
25. M. Ohsawa and W. Suetaka, *Corros. Sci.* **19** (1979) 709.
26. G. Trabanelli and V. Carassitti, *in* M.G. Fontana and R.W. Staehle (Eds), 'Advances in Corrosion Science and Technology' Vol. 1 (Plenum Press, New York, 1970), p. 147.
27. J.C. Marconato, L.O. Bulhes and M.L. Temperini, *Electrochim. Acta* **43** (1998) 771.
28. R. Haneda and K. Aramaki, *J. Electrochem. Soc.* **145** (1998) 1856.
29. R. Haneda, H. Nishihara and K. Aramaki, *J. Electrochem. Soc.* **144** (1997) 1215.
30. K. Suwa, T. Nishimoto, Y. Nagaoka and S. Aida, *Bull. Soc. Salt Sci. Jpn.* **15** (1961) 153.

31. Y. Yamamoto, H. Nishihara and K. Aramaki, *J. Electrochem. Soc.* **140** (1993) 436.
32. C. Miller, P. Cuendet and M. Gratzel, *J. Phys. Chem.* **95** (1991) 877.
33. C. Miller and M. Gratzel, *J. Phys. Chem.* **95** (1991) 5225.
34. Y. Yamamoto, H. Nischihara and K. Aramaki, *J. Electrochem. Soc.* **140** (1993) 2.
35. M. Itoh, H. Nishihara and K. Aramaki, *J. Electrochem. Soc.* **141** (1994) 8.
36. W.R. Thompson, M. Cai, M. Ho and J.E. Pemberton, *Langmuir* **13** (1997) 2291.
37. M. Itoh, H. Nishihara and K. Aramaki, *J. Electrochem. Soc.* **142** (1995) 6.
38. Y. Fend, W.-K. Teo, K.-S. Siow, Z. Gao, K.-L. Tan and A.-K. Hsieh, *J. Electrochem. Soc.* **144** (1997) 1.
39. H.P. Lee and K. Nobe, *J. Electrochem. Soc.* **133** (1986) 2035.
40. A.M. Beccaria and C. Bertolotto, *Electrochim. Acta* **42** (1997) 9.
41. S. Sankarapapavinasam and M.F. Ahmed, *J. Appl. Electrochem.* **22** (1990) 390.
42. R. Zvauya and J.L. Dawson, *J. Appl. Electrochem.* **24** (1994) 943.
43. L.H. Dubois and R.G. Nuzzo, *Annu. Rev. Phys.* **43** (1992) 437.
44. A. Morneau, A. Manivannan and C.R. Cabrera, *Langmuir* **10** (1994) 3940.
45. J. Wood and R. Sharman, *Langmuir* **10** (1994) 2307.
46. G. Che and C.R. Cabrera, *J. Electroanal. Chem.* **417** (1996) 155.
47. G. Che, A. Manivannan and C.R. Cabrera, *Physica A* **231** (1996) 304.
48. S.K. Jung and G.S. Wilson, *Anal. Chem.* **68** (1996) 591.
49. M. Itoh, H. Nishihara and K.J. Aramaki, *J. Electrochem. Soc.* **142** (1995) 3696.
50. W.R. Thompson and J.E. Pemberton, *Chem. Mater.* **7** (1995) 1309.